

Quantification of Horizontal Inhomogeneity in the Planetary Boundary Layer and its Impact on GNSS Radio Occultation Measurements

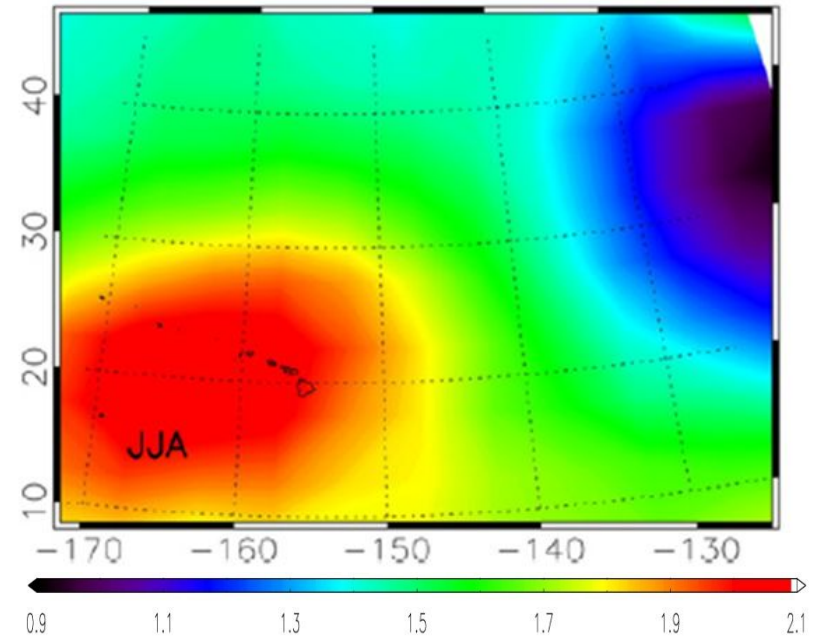
Thomas Winning¹,
Feiqin Xie^{1,2}, Kuo-Nung Wang², Chi.O. Ao²

¹Texas A&M University-Corpus Christi, Corpus Christi, TX

²Jet Propulsion Laboratory, Pasadena, CA

Motivation – Horizontal Inhomogeneity

- The GNSS Radio Occultation (RO) retrieval assumes local spherical symmetric atmosphere, which could be violated in the lower troposphere especially near PBL.
- How will the horizontal inhomogeneity (HI) affect the GNSS RO refractivity retrieval?
- What steps are needed to create a 2D atmospheric model to represent various levels of HI?

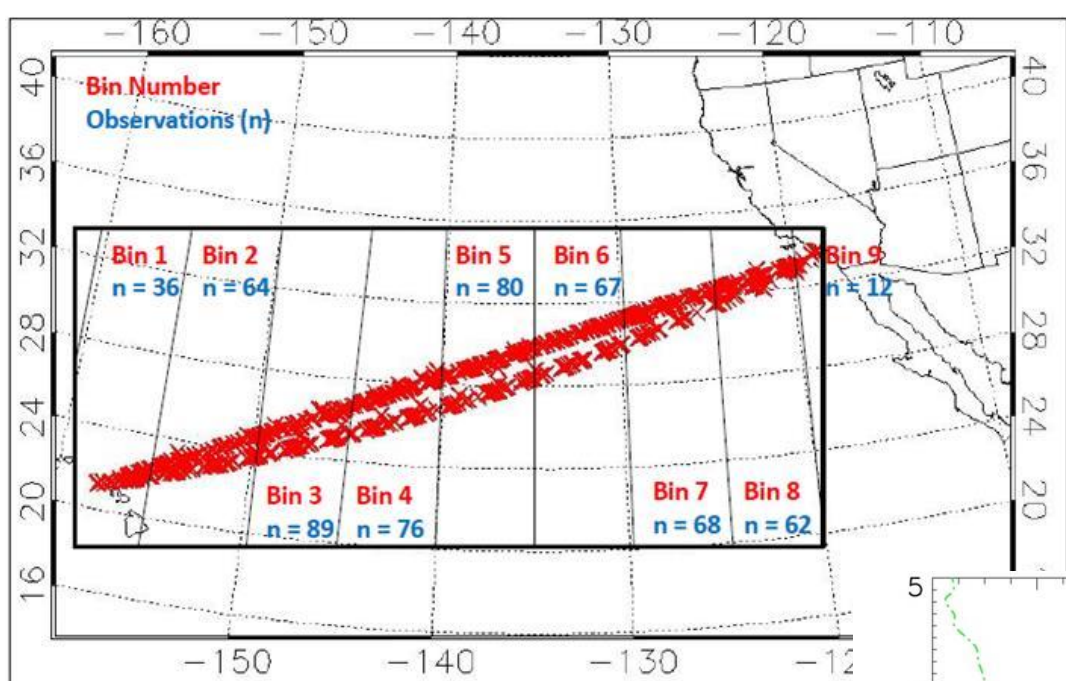


PBL height (km) climatology for JJA (2007-2012) using refractivity minimum gradient derived from COSMIC RO.

Objectives

- Build a 2D refractivity model to accommodate various levels of horizontal inhomogeneity (HI)
 - Create a simple 1D 3-segment N model
 - Validate with the MAGIC radiosonde observation over northeastern Pacific
 - Quantify the inhomogeneity (inhomogeneity index)
- Use multiple-phase-screen (MPS) simulator to mimic RO observations in the presence of 2D horizontal inhomogeneity
- Evaluate the impact of various levels of horizontal inhomogeneity on RO retrievals

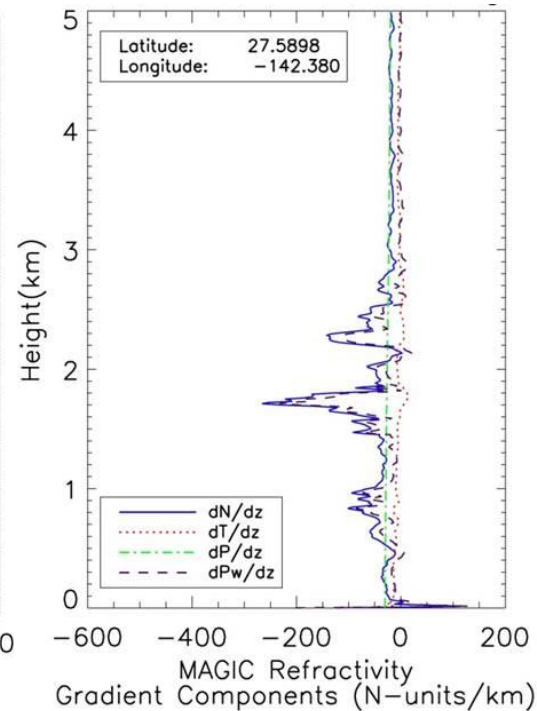
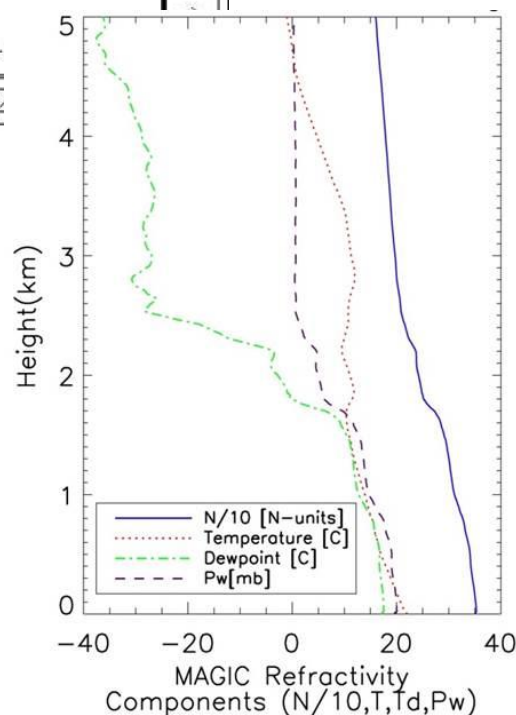
Transect over NE Pacific



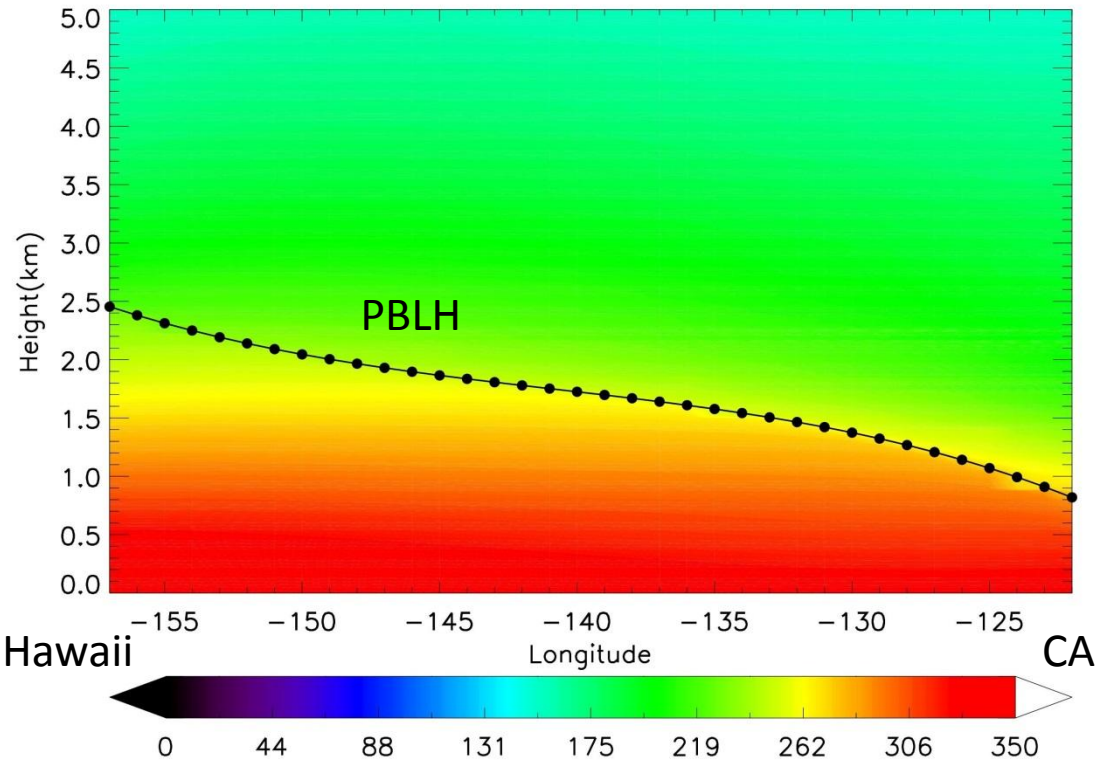
- Marine ARM GPCI investigation of Clouds-MAGIC
 - Los Angeles, California to Honolulu, Hawaii
 - October 2012-September 2013
 - Zhou et al., 2015

<https://www.arm.gov/sites/amf/mag>

- Top: MAGIC transect with location of radiosonde profiles
- Bottom left: Single profile showing temperature, dewpoint temperature, water vapor partial pressure and refractivity (N/10).
- Bottom right: gradient w.r.t. height of temperature, pressure, water vapor partial pressure and refractivity

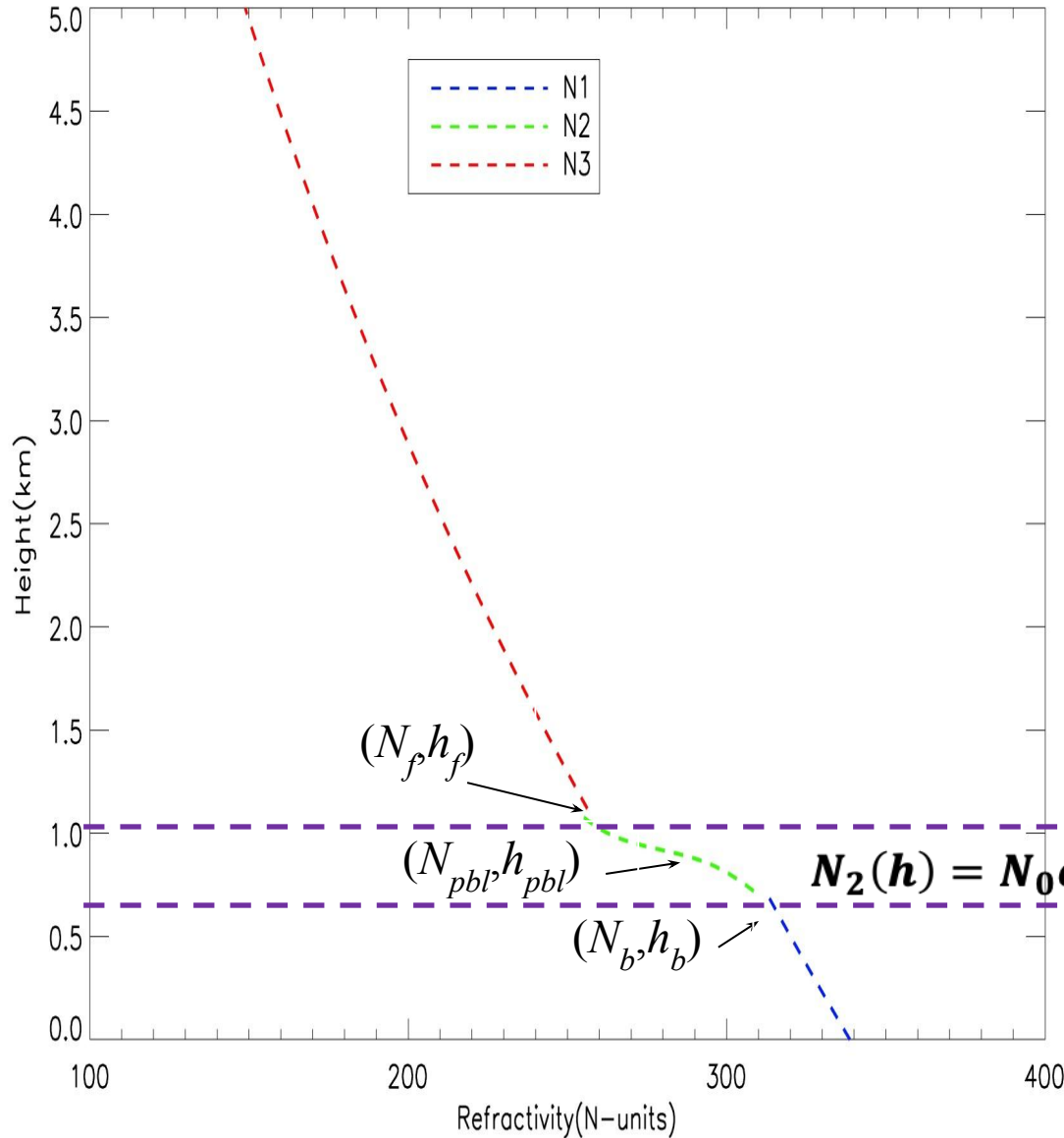


2D refractivity climatology over NE Pacific



- 2D refractivity field derived from MAGIC radiosonde soundings from 122°W to 157°W
- PBLH (height of minimum refractivity gradient) highlighted by black dotted line

1D 3-segment model profile



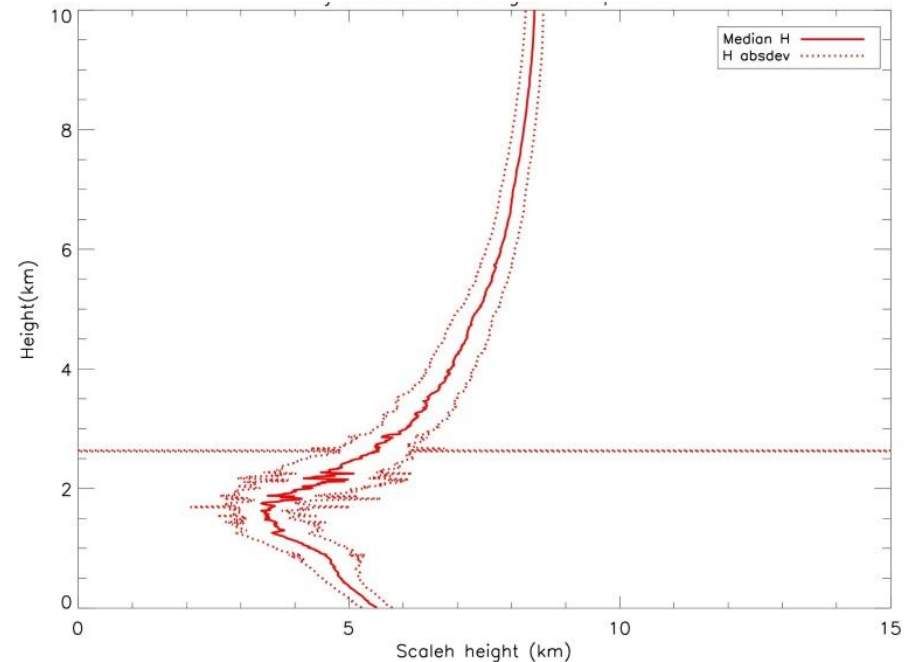
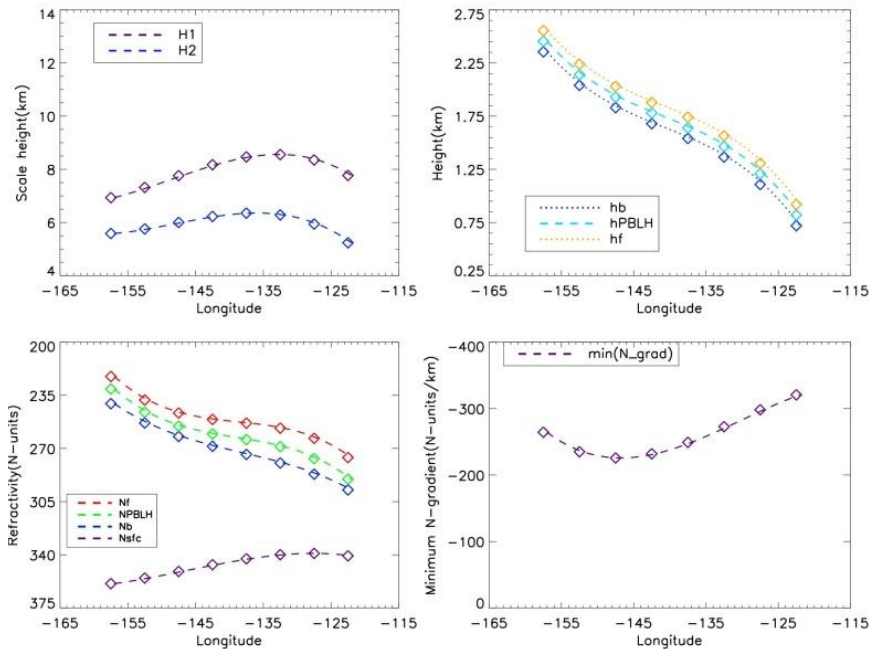
$$N_3(h) = N_f \exp\left(\frac{-(h-h_f)}{H_3(h)}\right)$$

$$N_2(h) = N_0 \exp\left(\frac{-h}{H_2}\right) \left[1 - A * \arctan\left(\frac{-(h-h_{pbl})}{B}\right) \right]$$

$$N_1(h) = N_{sfc} \exp\left(\frac{-h}{H_1}\right)$$

Model is a modified version of the parameterized equation from Sokolovskiy (2001)

Key variables for 1D refractivity model derived from MAGIC radiosondes



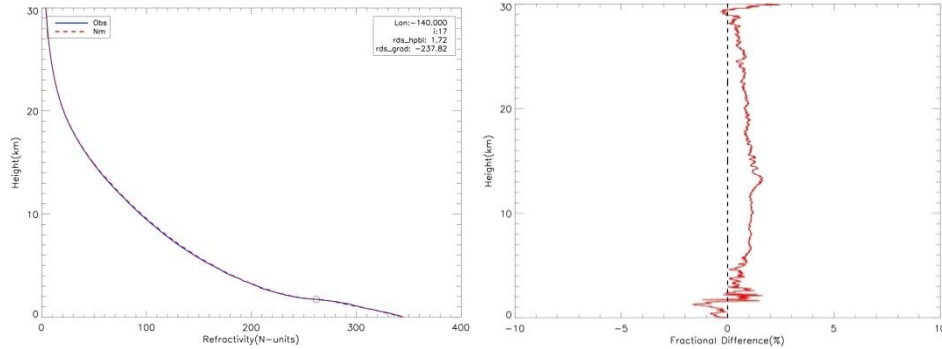
Scalar variables along NE Pacific transect.

Each variable is calculated from the median value of a 5° longitude and then interpolated to 1° horizontal resolution.

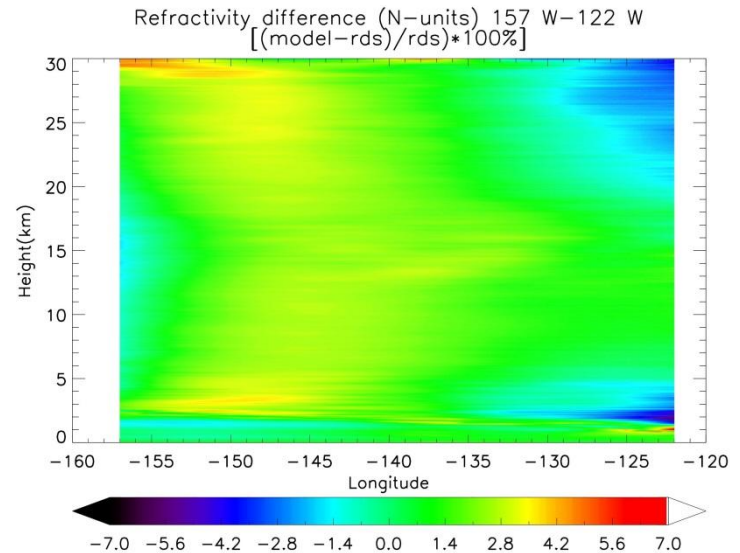
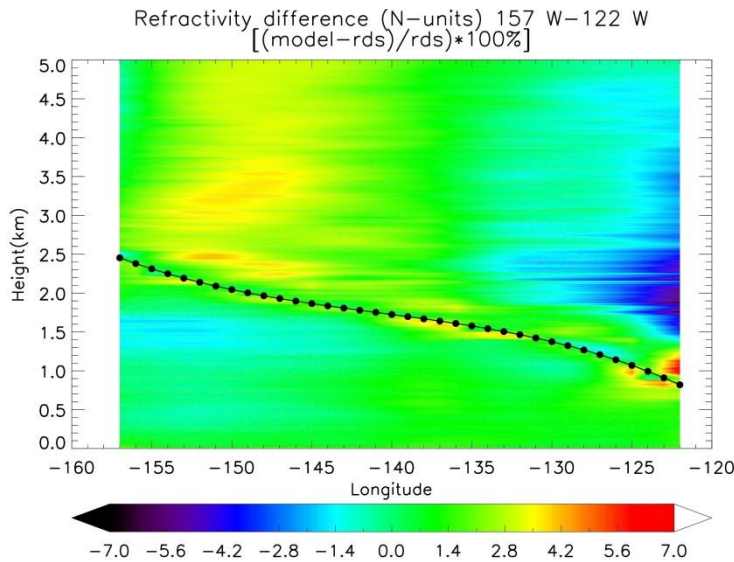
Data is then fit to a 3rd degree polynomial so each variable is a function of longitude and height.

Median scale height (solid red) \pm 1 absolute deviation, calculated from 36 1° median profiles

N-model vs. climatology



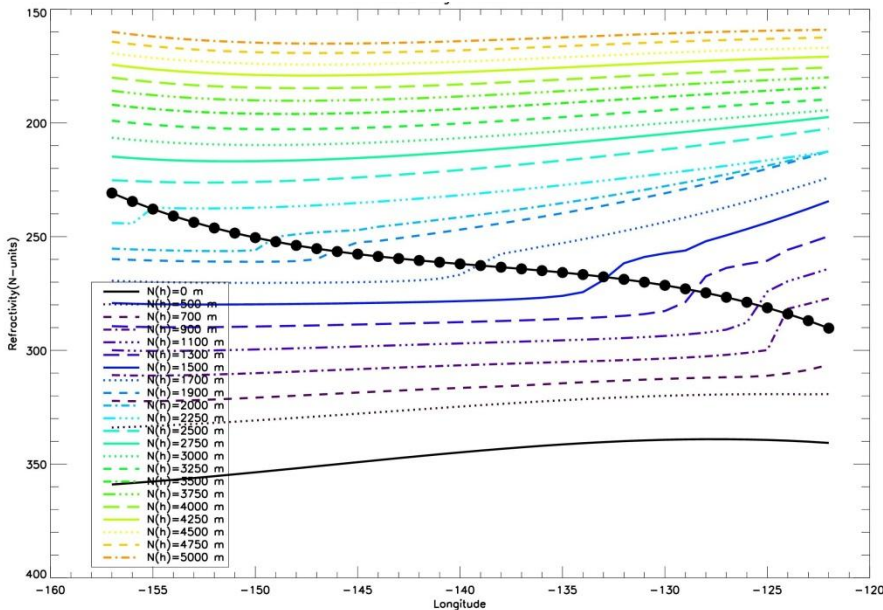
Left Figure: Surface to 30 km plot of N-model, radiosonde (solid blue) and Nm(dashed red).
 Right figure: Fractional difference between Nrds and Nm $((Nm-Nrds)/Nrds)*100\%$.



Fractional difference (%) between 2D Model and the radiosonde climatology for 0-5km (left) and 0-30km (right). Black dotted line (left) shows the PBLH

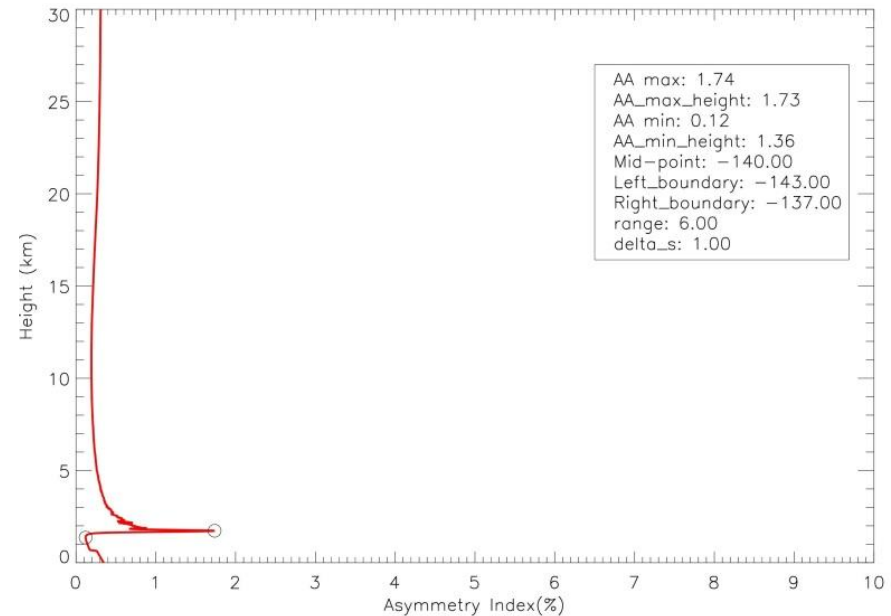
Quantifying inhomogeneity

- Asymmetry over analysis region



- Refractivity at constant height over analysis region
- Height intervals of 200 m from surface to 2 km increase to every 250 m from 2 km to 5 km
- Black connected circles represent the refractivity value at PBL
- Highlights the greatest asymmetry along the entire transect exists at the height of the PBL.

- Asymmetry index at $-140^\circ \pm 3^\circ$



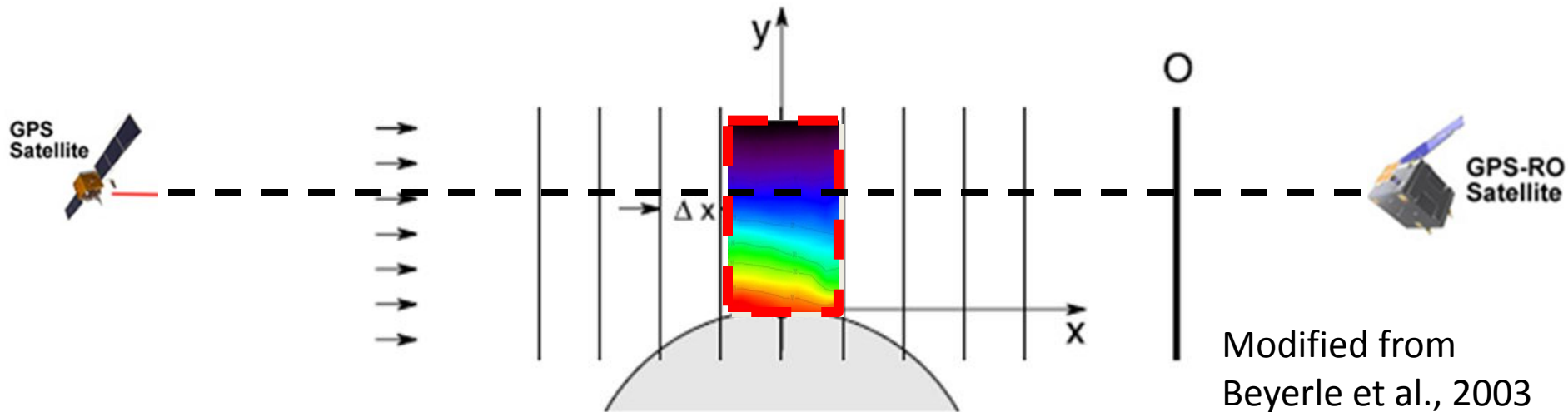
- Cross section total refractivity (CSTR)

$$CSTR = \int_{LB}^{RB} N(h_i) ds = \int_{LB}^{MPT} N(h_i) ds + \int_{MPT}^{RB} N(h_i) ds$$
- Cross section asymmetry (CSA)

$$CSA = \left| \int_{LB}^{MPT} N(h_i) ds - \int_{MPT}^{RB} N(h_i) ds \right|$$
- Cross section asymmetry index (CSAI)

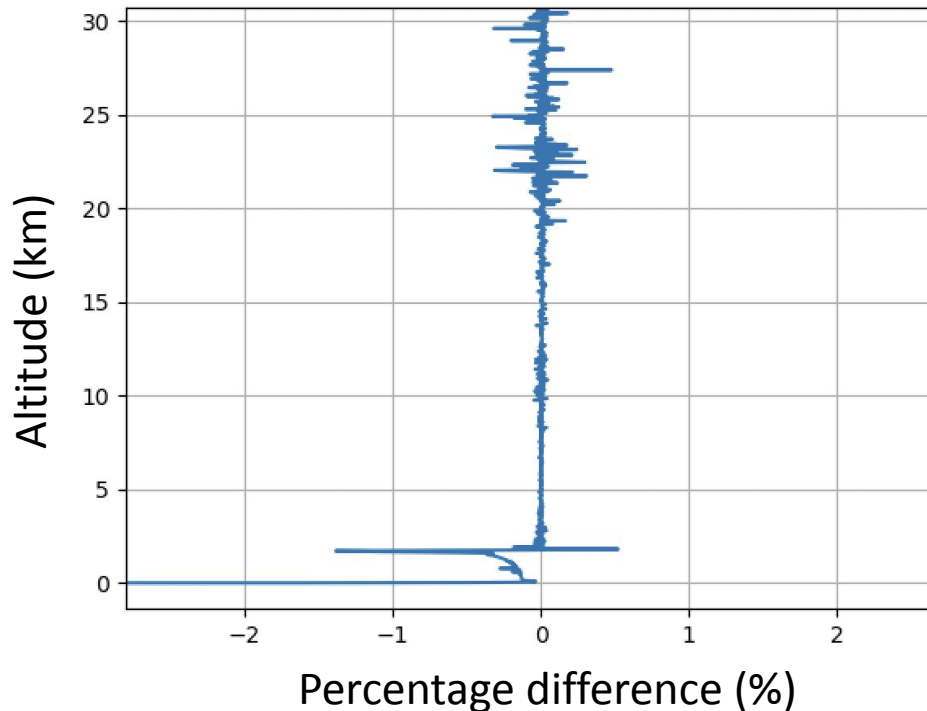
$$CSAI = \left(\frac{CSA}{CSTR} \right) 10^2, \text{ where: } 0 \leq CSAI \leq 10$$

Multiple Phase Screen Simulator



- Fourier split step solution of the parabolic wave equation
- Atmosphere approximated by a series of phase screens
- Full-wave diffraction effects with no required special treatment for multipath
- Key parameters for MPS
 - Center longitude: -140°
 - Longitude range: $x=-1000$ to $x=1000$ corresponding to $x= -150^\circ$ to $x= -130^\circ$
 - Screen interval (Δx): 1 km
 - Total number of screens: 2000
 - Vertical range: -250 m to 60 km

Retrieval vs. input



- Calculation of percentage difference between N retrieval (N_{ret}) and profile from center of domain (N_{-140}).
 - $((N_{ret}-N_{-140})/N_{-140}) * 100\%$
- Comparison at center of domain (-140°)
 - Bending could cause drift which is a reasonable explanation for the difference within the PBL.

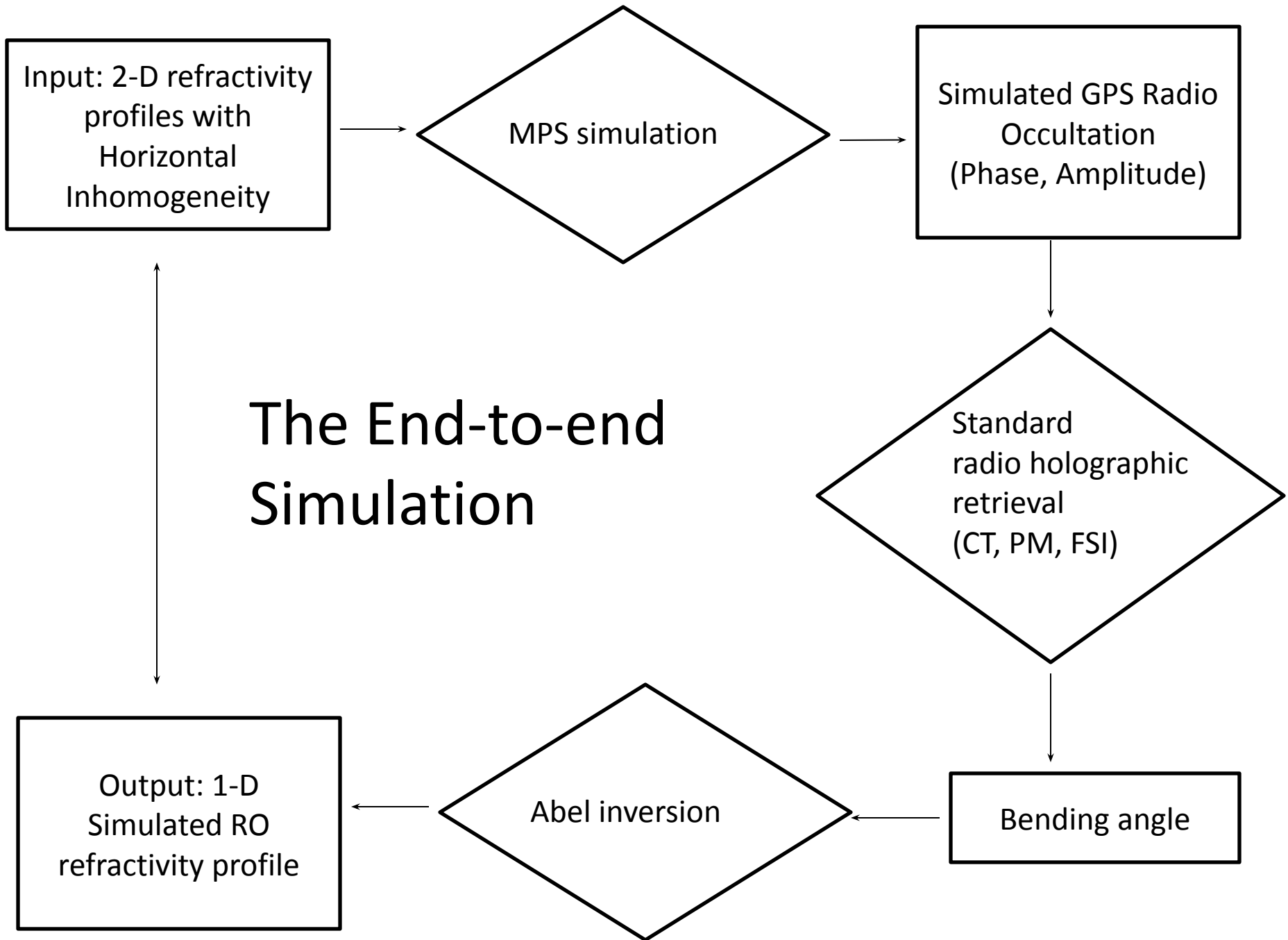
Conclusions and future work

- Work to date
 - A 2D refractivity model is created and validated by radiosonde data over NE Pacific. The 2D model can accommodate variation of inhomogeneity levels.
 - Inhomogeneity is quantified over the NE Pacific along the transect between South California and Hawaii using the asymmetry index.
 - MPS simulation is carried out to simulate the RO event in the presence of 2D horizontal inhomogeneity.
- Future work
 - Alter MPS simulation within the analysis region and evaluate the differences between simulation results.
 - Consider other variables that factor into the difference between the retrieval and model profile and how to isolate their contribution (ex. representative error, ducting-induced bias etc.)
 - Evaluate scenarios with varying inhomogeneity levels

Acknowledgements

- NASA project (NNX15AQ17G)
- Dr. Chi O. Ao and Dr. Kuo-Nung (Eric) Wang at JPL for help with MPS simulation
- Partial support
 - JPL subcontract
 - JPL-Summer Intern Program, 2016

QUESTIONS?



References

- Anthes, R.A., and coauthors, 2008. The COSMIC/FORMOSAT-3 Mission: Early Results. *Bull. Am. Meteorol. Soc.*, **89**, 313-333, doi:10.1175/BAMS-89-3-313
- Ao, C.O., Waliser, D.E., Chan, S.K., Li, J.-L., Tian, B., Xie, F., and Mannucci, A.J., 2012. Planetary boundary layer heights from GPS radio occultation refractivity and humidity profiles. *J. Geophys. Res.*, **117**, D16117. doi:10.1029/2012JD017598
- Beyerle, G., Gorbunov, M.E., and Ao, C.O. 2003. Simulation studies of GPS radio occultation measurements. *Radio Sci.*, **38**(5), 1084, doi:10.1029/2002RS002800
- Dee, D.P., and coauthors, 2011. The ERA-Interim reanalysis: Configuration and performance of the data assimilation system. *Q. J. R. Meteorol. Soc.*, 553-597, doi:10.1002/qj.828
- Fjeldbo, G. and Eshleman, V.R. 1968. The atmosphere of Mars analyzed by integral inversion of the Mariner IV occultation data. *Planet. Space Sci.*, **16**, 1035-1059
- Kursinski et al., 1997 Observing Earth's atmosphere with radio occultation measurements using the Global Positioning System. *JGR*, vol. **102**,D19, pgs. 23,459-23,465
- Malkus, J. S. 1958. On the structure of the trade wind moist layer, *Papers in Physical Oceanography and Meteorology*, **13** (2), 1-47. doi: 10.1575/1912/5443
- Smith, E.K., and Weintraub, S., 1953. The constants in the equation for atmospheric refractive index at radio frequencies. *Proc. IRE*, **41**, 39-41. doi:10.1109/JRPROC.1953.274297
- Sokolovskiy, S.V., 2001. Modeling and inverting radio occultation signals in the moist troposphere. *Radio Sci.*, **35** (3), 441-458. doi: 10.1029/1999RS002273
- Xie, F., Wu, D.L., Ao, C.O., Mannucci, A.J., and Kursinski, E.R., 2012. Advances and limitations of atmospheric boundary layer observations with GPS occultation over southeast Pacific Ocean. *Atmos. Chem. Phys.*, **12**, 903-918. doi:10.5194/acp-12-903-2012
- Zhou, X., Kollias, P., and Lewis, E.R., 2015. Clouds, Precipitation, and Marine Boundary Layer Structure during the MAGI Field Campaign. *J. Climate*, **28**, 2420-2442. doi: 10/1175/JCLI-D-14-00320.1